American Journal of Materials Science 2012, 2(4): 105-109
DOI: 10.5923/j.materials.20120204.02

Biomimetic Mineralization of $BaCO_3$ Microstructures By Simple CO_2 Diffusion Method

B. Sreedhar[1], Ch. Satya Vani[2], D. Keerthi Devi[1], V. Sreeram[3], M. V. Basaveswara Rao[3,*]

[1]Inorganic and Physical Chemistry Division, Indian Institute of Chemical Technology (Council of Scientific and Industrial Research), Hyderabad, Andhra Pradesh, 500607, India
[2]Department of Chemistry, SR International Institute of Technology, Rampally, Keesara (M), RR District, Andhra Pradesh, 501301, India
[3]Department of Chemistry, Krishna University, Machilipatnam, Andhra Pradesh, 521001, India

Abstract Barium carbonate ($BaCO_3$) microstructures have been synthesized in aqueous solution under ambient conditions with PABA (*p*-amino benzoic acid) and HEEDTA (N-(2 hydroxyethyl) ethylenediamine-N, N', N'' - triacetic acid) as simple additives. In this study we demonstrate that the integration of both the additives, PABA and HEEDTA under different experimental conditions, such as crystallization sites and pH will extend the possibilities for controlling the shape and size on microstructures of the inorganic crystals by means of a slow CO_2 simple diffusion route. The influence of variation of pH condition with two different additives on the particle size and morphology was investigated. Scanning electron microscopy, Fourier transform infrared spectroscopy and X-ray powder diffractometry were used to characterize the products. The results indicate that bunch like dendritic and limpet teeth shaped, $BaCO_3$ microstructures were obtained. Increasing pH led to the separation of rods from the complex structures.

Keywords Barium Carbonate, *P*-Amino Benzoic Acid, N-(2hydroxyethyl) Ethylenediamine-N, N', N'' - Triacetic Acid and Biomineralization

1. Introduction

Highly ordered complex structures have been studied extensively due to their unique nature and fantastic properties different from those of the monomorph structures[1]. For this, biomimetic synthesis of inorganic materials with complex and heirarchial structures, templates or organic additives with complex functionalization patterns are used to control the nucleation growth and alignment of inorganic crystals.

Researchers are increasingly concerned with the synthesis of advanced materials with enhanced properties. The use of inorganic-organic interface for the morphosynthesis of inorganic materials is an emerging soft chemical route[2]. The molecular interactions between inorganic - organic interface seem to control nucleation and growth which often stabilizing new modifications and morphologies[3]. Carbonate minerals like $CaCO_3$, $BaCO_3$, and $SrCO_3$, were intensively studied as a model compound for biomimetic mineralization[4]. $BaCO_3$ is having close resemblance with the aragonite type mineral with many industrial applications in the ceramic and glass industries as well as its use as a precursor for magnetic ferrites and/or ferroelectric materials[5]. Barium carbonate ($BaCO_3$) is also used as aprecursor for producing superconductor and ceramic materials[6] and other important applications in optical glass and electric condensers[7]. Various morphologies such as helical $BaCO_3$ fibers[8,9] candy-like, needle like or olivary like[10], nanofibers and rod like structures[11] in the presence of different additives are reported. In literature different biomimetic approaches to control the morphology of carbonate systems using a variety of additives/templates, such as Langmuir films[12-14], ultrathin organic films[15], self assembled monolayers[16-18], varied soluble additives like synthetic peptides[19], dendrimers[20,21], nicotinic acid[22], H_5hpdta, H_3heidi[23], PABA[24] and common polymers[25,26] have been described.

Here in, we present a study, on the biomimetic synthesis of $BaCO_3$ crystals by using two different organic additives, namely PABA and HEEDTA with simple CO_2 gas slow diffusion technique to prepare dendritic and limpet teeth shaped $BaCO_3$ structures, respectively in aqueous solution. However, to the best of our knowledge, limpet–teeth like $BaCO_3$ structures have not been reported till now.

2. Experimental

2.1. Materials and instruments

Para-aminobenzoicacid ($C_7H_7O_2N$), N-(2hydroxyethyl) ethylenediamine-N, N', N''-triaceticacid ($C_{10}H_{18}O_7N_2$),

* Corresponding author:
vbrmandava@yahoo.com (M.V. Basaveswara Rao)
Published online at http://journal.sapub.org/materials

ammonium carbonate $(NH_4)_2CO_3$, sodium hydroxide (NaOH) and barium chloride ($BaCl_2$) were of analytical grade and used without further purification. Double distilled water was used in all experiments.

2.2. Materials

X-ray diffraction measurements of the barium carbonate hierarchial structures were recorded using a Rigaku diffractometer (Cu radiation, λ = 0.1546 nm) running at 40 kV and 40 mA (Tokyo, Japan). FT-IR spectra of $BaCO_3$ structures were recorded with a Thermo Nicolet Nexus (Washington, USA) 670 spectrophotometer. The crystals were collected on a round cover glass (1.2 cm), washed with deionized water and dried in a desiccator at room temperature. The cover glass was then mounted on a SEM stub and coated with gold for SEM analysis.

2.3. Synthesis of $BaCO_3$ Crystals

A typical procedure for preparation of crystalline $BaCO_3$ crystals was carried out as follows: 2.5 mmol $BaCl_2$, 0.1 mmol PABA/HEEDTA were dissolved in 20 mL H_2O, prepared in a glass bottle and stirred continuously for complete dissolution. Then the pH of the solution was adjusted to 7.0 and 10.0 by using dilute NaOH. After that the prepared solution was then covered with parafilm which was punched with three needle holes and placed in larger desiccator containing crushed ammonium carbonate at the bottom. After 24hr crystallization, the parafilm was removed and the white precipitate deposited on the glass bottle rinsed with distilled water and ethanol and allowed to dry at roomtemperature for further crystallization.

3. Results

3.1. Structural Characterization of $BaCO_3$ Crystals

The crystal structures and the phase purity of the materials were determined by X-ray diffraction (XRD). XRD patterns of the as-prepared dendritic and limpet teeth shaped $BaCO_3$ microstructures at two different pH conditions – 7 and 10 are presented in Figures 1 and 2. All the observed diffraction peaks of the products can be attributed to pure orthorhombic $BaCO_3$ crystals (JCPDS card number: 71-2394). In Figure 1, the pattern of $BaCO_3$ crystals obtained in PABA solution displays the following diffraction peaks with (hkl) indices (110), (020), (111), (021), (002), (112), (200), (220), (221) (041), (202), (132), and (113). In Figure 2, the pattern of $BaCO_3$ crystals obtained in HEEDTA solution displays the following diffraction peaks with (hkl) indices (110), (020), (111), (021), (002), (112), (200), (220), (221), (132), and (113), of pure orthorhombic witherite phase. It may also be seen that the peak at (111) is the strongest, suggesting that $BaCO_3$ crystals obtained with PABA and HEEDTA aqueous solutions were well oriented and grew mainly along the crystallographic C-axis. This result was also maintained by SEM observation, which exhibited the dendrite and limpet teeth morphology of complex hierarchical structures. All of these complex microstructures were composed of microrods with diameters in the range of 1µm – 1.5µm. In comparison with Figures 1 (a)-(c), the pattern in Figures 2 a-2c has three changes. One is that two new diffraction peaks, (041) and (202) faces appear, and the second is that the relative intensity of (112), (200) planes are decreased at initial pH 3 and raised pH 10. The third main difference is the resolution of (021) as separate peak next to (111). This suggests that PABA and HEEDTA have different influence on the crystal growth of $BaCO_3$ which also can be interpreted by the fact that the two organic molecules can adsorb onto certain crystal faces $BaCO_3$ crystals and influence the crystal growth process.

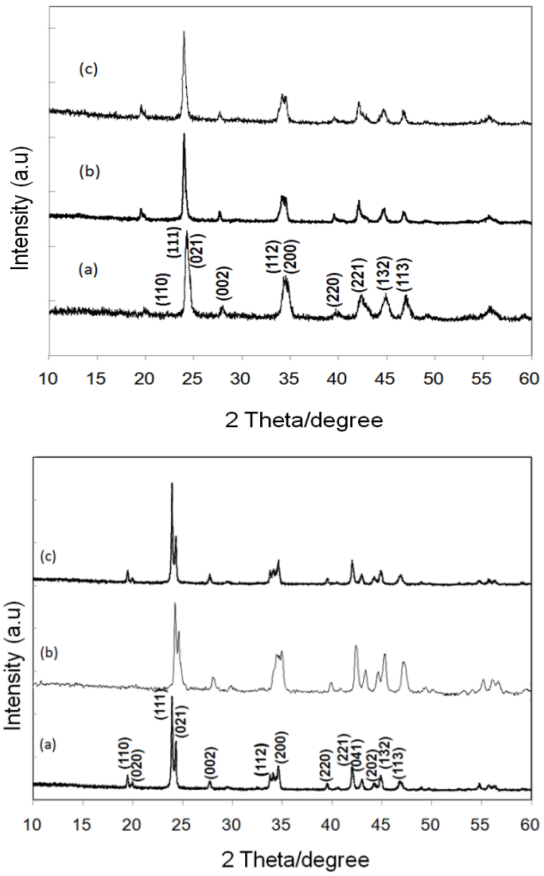

Figure 1. XRD pattern of $BaCO_3$ in the presence of PABA 1 (a) pH 3.0, (b) pH 7.0 and (c) pH 10.0. **Figure 2**.XRD pattern of $BaCO_3$ in the presence of HEEDTA 2 (a) pH 3.0; (b) pH 7.0, and (c) pH 10.0

3.2. Influence of Additives on the Morphology of $BaCO_3$

Significant changes in the morphologies were observed when the pH of the reaction conditions were varied – 7 and 10. Figure 3 and 4 show the SEM images of $BaCO_3$ structures obtained before and after adding the additives PABA and HEEDTA, respectively at initial pH(3.0) and rised pH(7.0 and 10.0) conditions. As can be seen From Figure 3a, and 4a, $BaCO_3$ microrods are obtained in the absence of additive, while in the presence of PABA at starting pH 3.0(without rising with NaOH), bunch like dendritic structures were observed (Figure 3b). From the magnified image

it can be clearly seen that the branch like product are built up of much smaller size subunits shown as inset in Figure 3b. No changes were observed in the morphology when the pH of the reaction mixture was increased to 7, except an increase in the length of the dendritic structures as shown in Figure 3c. On further increasing the pH to 10.0, the bunch like dendritic structures are separated and become almost twin shaped rods. As can be seen, at all the three different pH conditions, similar morphological changes with variation in the length of the dendritic structures were identified. Figure 4 shows the SEM images of $BaCO_3$ structures in the presence of the additive HEEDTA. Significant changes in the morphology was observed with this additive and the shape of $BaCO_3$ structures changed from rods to limpet teeth which is isostructural with the mineral aragonite, with sizes ranging from several micrometers to several tens of micrometers. At initial pH 3.0 more branches with long rods and sharp tips are observed. At neutral pH, short sized rods with less number of branches that are dispersed are seen. At pH 10.0, morphology of the $BaCO_3$ structures appears similar to that observed at initial pH 3. Moreover, the tips of the rods are not too sharp as seen in initial pH 3.0. So it can be concluded that, even though the morphology at different pH remain same, variation in the branching and size of the subunits is observed in the controlled experiments through the slow gas diffusion method.

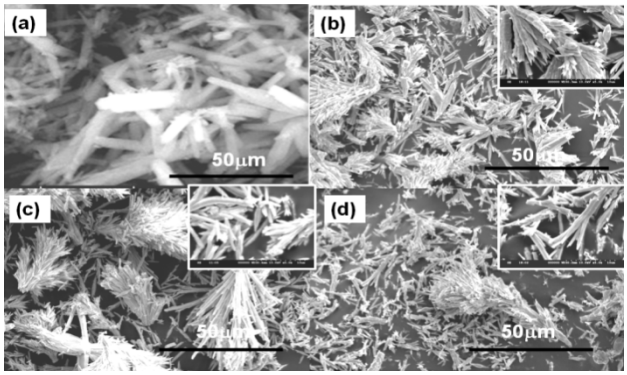

Figure 3. SEM images of $BaCO_3$ in the presence of PABA at varied pH conditions (a) absence of PABA, (b) initial pH 3.0, (c) pH 7.0, and (d) pH 10.0.

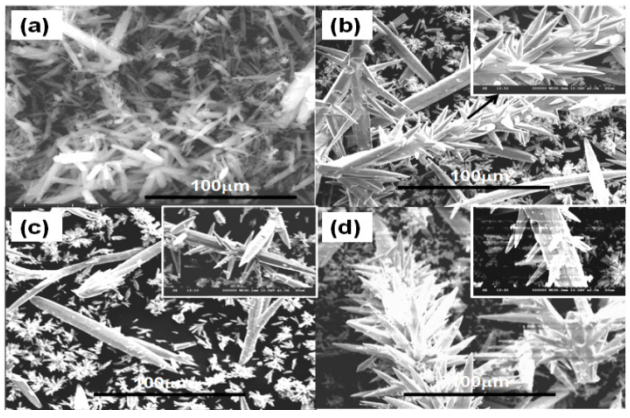

Figure 4. SEM images of $BaCO_3$ in the presence of HEEDTA at varied pH conditions (a) absence of HEEDTA, (b) initial pH 3.0, (c) pH 7.0, and (d) pH 10.0.

From the above morphology evolvement, we could clearly see the important role of PABA and HEEDTA under varied conditions during the crystal formation and growth process. The growth process of the branch like dendrites and limpet-teeth like morphology was carefully followed by pH-dependent experiments. SEM images of the products with different reaction time showed an obvious growth process from rods to bunch like dendrite units with PABA and rods to limpet teeth with HEEDTA. Figure 3 and 4 summarizes all major steps and changes involved in the formation of the $BaCO_3$ complex structures. However, it has to be pointed out that the exact growth mechanism is still unknown, although some explanation was given in the literature based on the role of intrinsic electric fields which direct the growth of dipole crystals[27-29].

3.3. FT-IR Analysis

To identify the growth mechanism and the effect of PABA and HEEDTA on $BaCO_3$ microstructures, the sample was analyzed by FT-IR spectroscopy. The IR bands at 1445 cm^{-1} (Figure 5b), and 1435 cm^{-1} (Figure 5c) correspond to the asymmetric stretching mode of C-O bond, while the weak band at 1059 cm^{-1} (Figure 5b, c) is attributed to the symmetric C-O stretching vibration. The weak bands at 1165 and 1059 cm^{-1} are C-H in-plane bending vibrations and the small peaks between 1500 cm^{-1} to 1400 cm^{-1} are C-C stretching vibrations in aromatic ring (Figure 5b). The extra peaks in Figure 5b and 5c are attributed to the functional groups (-COOH, NH_2, OH) that are present in the additives. In comparison with Figures 5b, the C-O stretching vibration peak around 1435 cm^{-1} in Figure 5c, shifts to lower frequency by 10 cm^{-1} (1445 cm^{-1}), suggesting that PABA and HEEDTA have different influence of $BaCO_3$. This is probably due to the fact that the two organic molecules can adsorb onto the different planes of $BaCO_3$ nuclei and influence the mode of crystal growth, resulting in little change of microstructure.

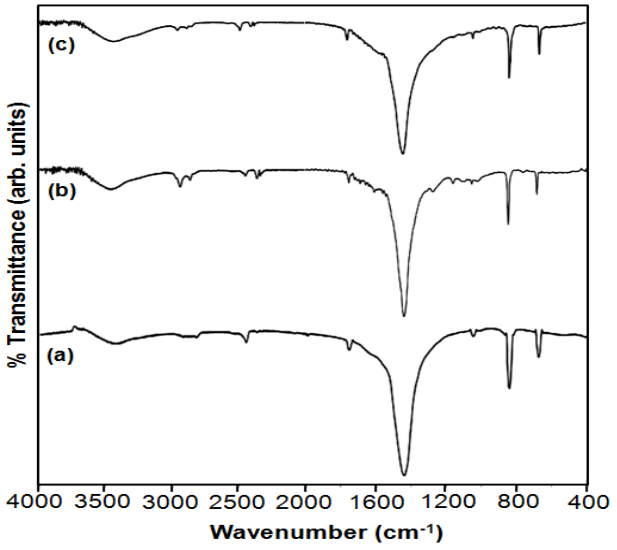

Figure 5. FT-IR of $BaCO_3$ microstructures nucleated (a) in the absence of an additive, (b) presence of PABA, and (c) presence of HEEDTA.

4. Discussion

On the basis of SEM observation, the growth mechanism for the generation of $BaCO_3$ complex structures can be described as rod to dendritic like structures and rod to limpet teeth shaped progression for PABA and HEEDTA, respectively. The first stage is the nucleation process that is the initial reaction between Ba^{2+} and amino/ carboxylic anions in PABA and hydroxyl/carboxylic anions in HEEDTA, which generates the $BaCO_3$ nuclei. The second stage is the formation of $BaCO_3$ rods via orientation growth along the crystallographic c-axis, as demonstrated by XRD. The third stage involves the formation of branches at the ends of the primary rod in PABA whereas with HEEDTA all over the branches on the primary rod leading to the formation of bunch like dendritic structures or limpet teeth like $BaCO_3$ microstructures. The results above show that PABA promotes the formation of branch like dendritic structures while HEEDTA favors the formation of limpet teeth like $BaCO_3$ crystals. So it can be presumed that the amino and/or carboxylic anions in PABA and hydroxyl and/or carboxyl anions in HEEDTA control the formation of microstructures by adsorbing onto certain facets of $BaCO_3$ crystals.

5. Conclusions

Different morphologies of $BaCO_3$ complex structures were controlled by the cooperation of the PABA and HEEDTA additives by means of a slow CO_2 simple diffusion technique. It is noticeable that the pH variation with both the different organic additives has remarkable effect on the morphology. In this system pH and additive is the key factor for the biomineralisation research and development of new materials which could find various applications.

REFERENCES

[1] X. X. Xu, X. Wang, A. Nisar, X. Liang, J. Zhuang. S. Hu, and Y. Zhuang., 2008, Combinatorial Hierarchically Ordered 2D Architectures Self-assembled from Nanocrystal Building Blocks, Adv. Mater. 20(19), 3702-3708.

[2] S. Mann, D. D. Archibald, J. M. Didymus, B. R. Heywood, F. C. Meldrum and V. J. Wade., 1992, MRS Bull. 32.

[3] S. Mann, D. D. Archibald, and J. M. Didymus, T. Douglas, B. R. Heywood, F.C. Meldrum, and N. J. Reeves., 1993, Crystallization at Inorganic-organic Interfaces: Biominerals and Biomimetic Synthesis, Science 261, 1286-1292.

[4] W. Li, S. Sun, Q. Yu, and P. Wu., 2010, Controlling the Morphology of $BaCO_3$ Aggregates by Carboxymethyl Cellulose through Polymer Induced Needle-Stacking Self-Assembly, Cryst. Growth Des. 10(6), 2685-2692.

[5] A. Zelati, A. Amirabadizadeh, and A. Kompany., 2011, Preparation and Characterization of Barium Carbonate Nanoparticles, International Journal of Chemical Engineering and Applications, 2(4), 299-303.

[6] L. Chen, Y. Shen, A. Xie, J. Zhu, Z. Wu, and L. Yang., 2007, Nanosized barium carbonate particles stabilized by cetyltrimethylammonium bromide at the water/hexamethylene interface, Cryst. Res. Technol. 42(9), 886 – 889.

[7] D. Jin, X. Yu, L. Yue, and Ping Sun., 2009, Synthesis of $BaCO_3$ with Different Morphologies Using Amphiphilic PS–PAA Copolymer as Medium Inorganic Materials, 45(2), 168–172.

[8] J. H. Zhu, S. H. Yu, A. W. Xu, and H. Colfen., 2009, The biomimetic mineralization of double-stranded and cylindrical helical $BaCO_3$ nanofibres**,** Chem. Commun. 1106-1108.

[9] S. H. Yu, H. Colfen, H. K. Tauer, and M. Antonietti., 2005, Tectonic arrangement of $BaCO_3$ nanocrystals into helices induced by a racemic block copolymer, Nat. Mater. 4, 51-55.

[10] T. Wang, J. Mitchell, H. Borner, H. Colfen and M. Antonietti., 2010, $BaCO_3$ mesocrystals: new morphologies using peptide–polymer conjugates as crystallization modifiers, Phys. Chem. Chem. Phys. 12, 11984–11992.

[11] T. X. Wang, A. W. Xu, and H. Colfen., 2006, Formation of Self-Organized Dynamic Structure Patterns of Barium Carbonate Crystals in Polymer-Controlled Crystallization, Angew. Chem. Int. Ed. 45(27), 4451-4455.

[12] S. Mann, B. R. Heywood, S. Rajam, and S. J. D. Birchal., Controlled crystallization of $CaCO_3$ under stearic acid monolayers, Nature 1988, 334, 692-695.

[13] D. J. Ahn, A. Berman, and D. Charych., 1996, Probing the Dynamics of Template-Directed Calcite Crystallization with in Situ FTIR, J. Phys. Chem. 100(30), 12455-12461.

[14] A. L. Litvin, S. Valiyaveettil, D. L. Kaplan, and S. Mann., 1997, Template-directed synthesis of aragonite under supramolecular hydrogen-bonded langmuir monolayers, Adv. Mater. 9(2), 124-127.

[15] D. D. Archibald, S. B. Qadri, and B. P. Gaber., 1996, Modified Calcite Deposition Due to Ultrathin Organic Films on Silicon Substrates, Langmuir, 12(2), 538-546.

[16] J. Kuther, G. Nelles, R. Seshadri, M. Schaub, H.J. Butt, and W. Tremel., 1998, Templated Crystallisation of Calcium and Strontium Carbonates on Centred Rectangular Self-Assembled Monolayer Substrates**,** Chem. Eur. J. 4(9), 1834-1842.

[17] J. Aizenberg, A. J. Black, and G. M. Whitesides., 1999, Control of crystal nucleation by patterned self-assembled monolayers, Nature. 398, 495-498.

[18] J. Aizenberg, A. J. Black, and G. M. Whitesides., 1999, Oriented Growth of Calcite Controlled by Self-Assembled Monolayers of Functionalized Alkanethiols Supported on Gold and Silver, J. *Am. Chem. Soc.* 121(18), 4500-4509.

[19] D. B. DeOliveira, and R. A. Lauren., 1997, Control of Calcite Crystal Morphology by a Peptide Designed To Bind to a Specific Surface, J. *Am. Chem. Soc.* 119(44), 10627-10631.

[20] K. Naka, Y. Tanaka, Y. Chujo, and Y. Ito., 1999, The effect of an anionic starburst dendrimer on the crystallization of $CaCO_3$ in aqueous solution, Chem. Commun. 1931-1932.

[21] N. Naka. 2003, Top. Curr. Chem. 141**,** 228.

[22] C. Satyavani, K. Balakrishna, C. Rambabu, M. Saratchandra Babu., 2010, Influence of Vitamin B_3 on Morphosynthesis of

$CaCO_3$, $BaCO_3$ and $SrCO_3$ Micro and Nano Structures, J. Metallurgy and Materials Science. 52(4), 351-356.

[23] M. Saratchandra Babu, C. E. Anson and A. K. Powell., 2006, Modelling $CaCO_3$ Biomineralisation process, J. of Inorg. Biochem. 100, 1128.

[24] M. Saratchandra Babu, C. Satyavani, C. Rambabu and K. Sethuram., 2010, Biomimetic Growth of flower like calcite morphology, J. Mat. Sci. 7, 55.

[25] S. H. Yu, H. Colfen, A. W. Xu, and W. F. Dong., 2004, Complex Spherical $BaCO_3$ Superstructures Self-Assembled by a Facile Mineralization Process under Control of Simple Polyelectrolytes, Cryst. Growth Des. 4(1), 33-37.

[26] J. T. Han, X. Xu, D. H. Kim, and K. Cho., 2005, Biomimetic Fabrication of Vaterite Film from Amorphous Calcium Carbonate on Polymer Melt: Effect of Polymer Chain Mobility and Functionality, Chem.Mater. 17(1), 136-141.

[27] R. Kniep, and S. Busch., 1996, Biomimetic Growth and Self-Assembly of Fluorapatite Aggregates by Diffusion into Denatured Collagen Matrices, Angew. Chem. Int. Ed. Engl. 35(22), 2624-2626.

[28] S. Busch, H. Dolhaine, A. DuChesne, S. Heinz, O. Hochrein, F.Laeri, O.Podebrad,U.Vietze, T.Weiland, and R.Kniep.,1999, Biomimetic Morphogenesis of Fluorapatite-Gelatin Composites: Fractal Growth, the Question of Intrinsic Electric Fields, Core/Shell Assemblies, Hollow Spheres and Reorganization of Denatured Collagen, *Eur. J. Inorg. Chem*. 1999(10), 1643-1653.

[29] H. Colfen and L. Qi., 2001, Prog Colloid Polym. Sci. 11, 200.